Available online at www.sciencedirect.com
SCIENCE DIRECT
Journal of Photochemistry and Photobiology A: Chemistry 180 (2006) 282–288
Journal of Photochemistry and Photobiology A:Chemistry
www.elsevier.com/locate/jphotochem

Control strategies for reactive processes involving vibrationally hot product states

Dorothee Geppert *, Regina de Vivie-Riedle

LMU Department Chemie, Butenandt-Str. 11, 81377 München, Germany

Received 5 January 2006; received in revised form 10 February 2006; accepted 13 February 2006
Available online 6 March 2006

Abstract

We present an all optical control mechanism for the switching process in fulgides via electronically excited states in the presence of conical intersections. The underlying photoreaction is the ring opening or closure of the central C_6-ring chromophore. The control of this reaction is realized with shaped laser pulses which are obtained by Optimal Control Theory. Our implementation of the algorithm enables the definition of a target in the electronic ground state even if vibrationally hot product states are formed during the reaction demanding the appliance of a damping function. We introduce a flexible target definition including all parts of the wavepacket that will reach the target region within a given time interval *T*. Thereby the localization of the wavepacket inside this region at a specific point in time is not mandatory. A target definition in the ground state facilitates the comparability to experiments. With this target, the control algorithm favors an all optical process which is faster than the relaxation through the conical intersections. To enhance the possibility of experimental realizations, we analyze the optimized pump–dump sequence to allow a reconstruction and simplification of the laser field.

Keywords: Optimal Control Theory; Molecular switches; Flexible target definition; Control of reactive processes

1. Introduction

Fulgides are considered as promising candidates for molecular switches [1–3] which can be used as active devices in nanotechnology and for the implementation of logic gates in molecular computation. They are bistable and their isomers can be distinguished by their physical properties. When used as the bridging unit between an electron donor and acceptor moiety they offer the possibility to alter the system's properties by a specific photochemical reaction. In the open form E (see Fig. 1), energy or electron transfer is possible, while the closed form C suppresses fluorescence but leads to a fast radiation–less decay [2]. In our present investigations, we concentrate on the switching process between these two isomers which is initialized by a laser excitation in the UV/vis. For an effective switch a very high quantum yield is necessary, thus we suggest to enhance the yield by the use of shaped femtosecond laser pulses. We use Optimal Control Theory (OCT) to find these optimal laser pulses. In an iterative scheme, the shape of the laser field which guides the wavepacket from the initial to the target state is optimized [4–8]. In the experiment, the optimized pulses are found in closed loop set-ups based on genetic algorithms and are constructed by phase and frequency modulation [9–13].

The control of reactive photochemical systems like fulgides exhibits several challenges. Parts of the reaction occur in an optically not accessible dark region. This requires the generation of an excited state wavepacket with well-defined features like shape and momentum which subsequently evolves on the hypersurface to the target in the ground state. In photoreactions like in fulgides, where an ultrafast return to the ground state via conical intersections is possible, vibrationally hot molecules are formed during the reaction. Their numerical treatment becomes challenging in the OCT algorithm where forward and backward propagations are needed.

From an experimental point of view, the excitation frequency lying in the ultraviolet is a solvable but demanding task for pulse shaping [14,15]. Therefore we analyze the theoretically optimized pulse to extract the parts essential for the switching process. Based on this knowledge, we try to approximate the optimal field by a sequence of simpler Gaussian laser pulses.

* Corresponding author. Tel.: +49 89 2180 77535; fax: +49 89 2180 77133.
E-mail addresses: Dorothee.Geppert@cup.uni-muenchen.de (D. Geppert), Regina.de_Vivie@cup.uni-muenchen.de (R. de Vivie-Riedle).

1010-6030/$ – see front matter © 2006 Elsevier B.V. All rights reserved.
doi:10.1016/j.jphotochem.2006.02.017

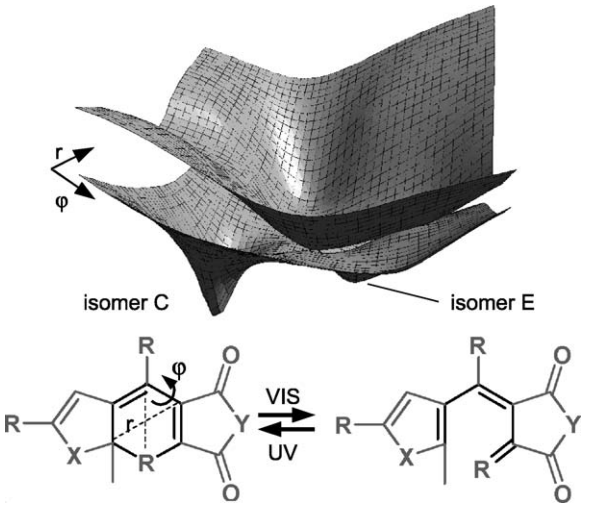

Fig. 1. The ring opening of a cyclohexadiene unit to an all-*cis* hexatriene unit constitutes the switching process of fulgides. The reactive coordinates r and φ are indicated. The two dimensional potential energy surfaces include both minima as well as two conical intersections connecting the excited state and the ground state.

2. The system under consideration

Fulgides exist in two stable isomers which can be swapped by a photochemical reaction (see Fig. 1). Their different absorption frequencies make them addressable individually and enable a selective read-out. The active center of these molecules consists of a cyclohexadiene/all-*cis* hexatriene subunit (indicated in black in Fig. 1). The opening or closure of this ring subunit is the decisive step in the switching process of the fulgides. Therefore we concentrate our investigations on the reaction of this subunit.

The ring opening of cyclohexadiene is a well known photochemical reaction following the Woodward–Hofmann rules that was studied experimentally [16–19] and theoretically [20–25]. After the excitation of cyclohexadiene the system evolves through various conical intersections leading to a branching into the ground states of both isomers cZc-hexatriene and cyclohexadiene which correspond to isomers E and C in fulgides, respectively. The following isomerizations of cZc-hexatriene to its more stable *trans*-isomers are not important for our considerations as they are sterically inhibited in fulgides. The most important features of this ring opening reaction can be described in two reactive coordinates r and φ (Fig. 1) introduced in [23]. The asymmetric squeezing of the ring is described by r and φ is the angle between the two indicated diagonals. There are two excited electronic states involved in the reaction. As it is known from experiments that the initially excited electronic state is depopulated completely within 10 fs [17], the coupling between these two states must be very strong. Therefore we treat the two crossing excited states as one adiabatic surface [25]. On the resulting potential energy surfaces, derived from interpolation between ab initio data points, we perform quantum dynamical calculations on a grid with the Chebychev propagation scheme [26,27]. The laser excitation is treated semi-classically and the effect of the conical intersections connecting the excited state with the ground state is calculated non-adiabatically with the coupling elements derived by quantum chemical calculations as described in [24]. In the following calculations, we regard the backward reaction, i.e. the ring closure from isomer E to isomer C.

3. Ground state target

The great challenge to control this reaction is made more difficult by the fact that parts of the excited state are not accessible by laser excitation. Only in the Franck–Condon regions of both isomers transition dipole moments of relevant size allow an optical transfer. Here a wavepacket must be prepared which subsequently propagates freely along the desired pathway. We could already demonstrate the control of this system within the framework of OCT in [25], where an intermediate target was used in the excited state. The intermediate target was a well-defined wavepacket with respect to magnitude and direction of momentum so that it evolved through a conical intersection to the desired target. This solution relies on a fast transfer through the conical intersections. However, this transfer is in general not completed in one step. Thus, the system has to reach the relevant conical intersection several times and a loss of control is inevitable if the conical intersections are located in an optically dark region as it is in this case. In addition, no direct experimental counterpart for the intermediate target is known so far. Therefore it is desirable to define the electronic ground state of the wanted isomer as the target state. If we try to do so, we encounter several challenges: after its return to the ground state through the conical intersections the wavepacket is vibrationally hot and its kinetic energy is high enough to reach the grid boundaries in the ground state. Due to the numerical implementation with periodic boundary conditions, the wavepacket must not evolve over the grid boundaries, but has to be damped away if it reaches them. In addition, we assume that the parts of the wavepacket which cross the minimum of isomer C will finally relax into this minimum. To mimic this process, the wavepacket is damped in the minimum of isomer C too, as there is no relaxation into other coordinates or a bath included in our system Hamiltonian. The real-valued damping function G, depicted in Fig. 2a), sets the corresponding parts of the wavefunction in the ground state to zero [28,29]. Thus, the damping function G is not connected to any dissipation process, but prevents the occurence of a non-physical reaction progress (e.g. switching to the other minimum in the ground state) by eliminating the affected parts of the wavepacket from the subsequent dynamical calculation. This damping process complicates the backward propagation needed in the optimal control algorithm. In OCT, the optimal laser field is found by simultaneous propagations of the initial wavefunction Ψ and the target wavefunction λ. Backward propagation becomes necessary because initial and final state are defined at different points in time, namely at $t=0$ and $t=T$ which is the maximum duration time of the laser field. When a spatial projection operator P is used to define the target region, the target wavefunction λ is built by letting P act on Ψ.

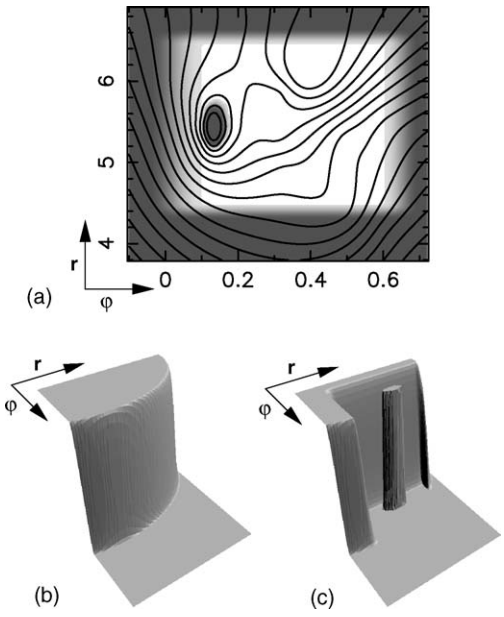

Fig. 2. (a) Ground state surface and damping function G (dark grey≙0, white≙1). The axes are given in Bohr. (b) The target operator P. (c) $(1-G)\,P$, parts of the ground state wavefunction in this region are saved for the backward propagation.

To enable the backward propagation, the damped parts are saved, similar to the approach in [30], where a cutoff function corresponding to our damping function was used at the grid boundaries. To match our conditions, three spatial operators are needed that act on the wavefunction in the electronic ground state (see Fig. 2): the damping function G, the projection operator P which defines the desired target region, and $(1-G)P$, which defines the parts of the wavefunction that have to be saved for the backward propagation. To avoid numerical fluctuations, one has to ensure that all these functions exhibit a smooth transition from one to zero, here provided by a $\sin^2(r, \varphi)$ function. The exact shape of G has no influence on the target yield.

We perform the optimizations according to the following scheme (cf. Fig. 3): after several timesteps dt the wavefunction $\Psi(t_n)$ is split into two parts: $G\Psi$ is propagated further, $(1-G)\Psi$ is split once more by P into parts in the target region which are saved and parts which are canceled out. For simplicity, in the Fig. 3 as well as in the following equations, we assume a splitting after every timestep:

$$\begin{aligned}|\Psi(t_n)\rangle &= G|\Psi(t_n)\rangle + (1-G)|\Psi(t_n)\rangle \\ &= G|\Psi(t_n)\rangle + P(1-G)|\Psi(t_n)\rangle \\ &\quad + (1-P)(1-G)|\Psi(t_n)\rangle. \end{aligned} \tag{1}$$

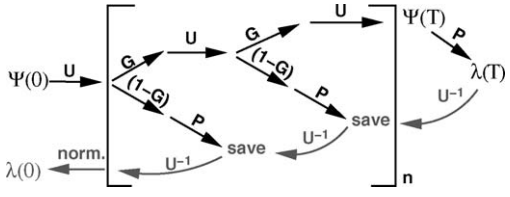

Fig. 3. Optimization scheme with a damping function G and a projection operator P.

At the selected final time of the propagation $t=T$, P operates on the remaining part of $\Psi(T)$, which leads to $\lambda(T)$. Because of the damping function, $||\lambda(T)||^2$ can be zero. The parts of Ψ that have reached the target region at earlier times are not included in $\lambda(T)$ and a normalization of the target wavefunction is not possible at this point in time. Therefore we do not use λ at time T to calculate the yield. For the same reasons, it is not advisable to calculate the electric field during a simultaneous backward propagation of Ψ and λ as it is usually done when a projection operator is used. Instead, we propagate λ back in time by using the backward propagator U^{-1} with the same laser field (reversed in time) and at the appropriate points in time, the saved parts $|\Phi_s\rangle = P(1-G)/\Psi\rangle$ are added:

$$\begin{aligned}&|\lambda(T)\rangle = P|\Phi(T)\rangle \\ &|\lambda(T-\mathrm{d}t)\rangle = U^{-1}|\lambda(T)\rangle + |\Phi_s(T-\mathrm{d}t)\rangle \\ &|\lambda(T-2\mathrm{d}t)\rangle = U^{-1}|\lambda(T-\mathrm{d}t)\rangle + |\Phi_s(T-2\mathrm{d}t)\rangle \\ &\vdots \\ &|\lambda(0)\rangle = U^{-1}|\lambda(\mathrm{d}t)\rangle + |\Phi_s(0)\rangle \end{aligned} \tag{2}$$

At time $t=0$, a normalization leads to a well-defined target wavefunction λ_{norm} and the total yield can be calculated, including now all parts of the wavefunction that will reach the target region during the propagation at any time $t \le T$. Then, Ψ and λ_{norm} are propagated forward, λ_{norm} with the same laser field ε^k, Ψ with the new laser field ε^{k+1}, calculated during this simultaneous propagation:

$$\varepsilon^{k+1} = \frac{-s(t)}{\alpha_0}\mathrm{Im}\langle\lambda^k_{\mathrm{norm}}(t)|\mu|\Psi^{k+1}(t)\rangle \tag{3}$$

Here again, $\Psi^{k+1}(t)$ is splitted into three parts and $|\Phi^{k+1}_s(t)\rangle = P(1-G)|\Psi^{k+1}(t)\rangle$ is saved for the backward propagation and to allow the target definition in the next iteration step.

4. Control of the product yield

With this new optimization scheme, we implement in the OCT formalism a target definition on the ground state for photochemically driven reactive processes. In the following calculation, the initial wavefunction $|\Psi(0)\rangle$ is the vibrational ground state of isomer E and the target definition is the part of the electronic ground state belonging to isomer C (see Fig. 2b)). As realized in our case (Fig. 2), the target can now be defined inside and/or outside the region of the damping function.

After the photo excitation, the wavepacket leaves the Franck–Condon region very fast, the only region where its motion can be controlled by laser light. It enters the dark region including the conical intersections where no further manipulation is possible. When the return to the ground state takes place via the conical intersections, we already showed that the relaxation does not occur in one rush, but in a stepwise process. An alternative mechanism would be an all optical process like a pump–dump scheme [31] which is a fast and effective process. In addition, this process is very appropriate for the optimal control algorithm, as it is the optical process which is directly addressable by the OCT algorithm. In comparison, the conical

intersections are a feature of the system that cannot be controlled but has to be used as it is. For clarification, consider Eq. (3), where the formula for the optimized field is given: the dipole moment connects the ground state of the initial wavefunction with the excited state of the target wavefunction (i.e. the Lagrange multiplier) and vice versa. When $\Psi(t)$ or $\lambda(t)$ propagate across a dark region, where the transition dipole moment is zero, the electric field becomes zero, too. Potential features inside this region therefore have only indirect influence on the optimal field.

Other scenarios are possible, e.g. Fujimura and co-workers [32] have recently demonstrated the control of the *cis–trans* isomerization of rhodopsin where the optimized pulse makes use of the conical intersection by guiding the wavepacket in a localized manner through it. In their example the conical intersection does not lie in a dark region and the coupling between the electronic surfaces is so strong, that almost all of the excited wavepacket changes the adiabatic surface when it reaches the conical intersection.

Our experience with the ringopening system, where the conical intersections lie in a dark region, shows that here the algorithm rarely takes advantage of the conical intersections, but usually prefers the faster optical way. However, a necessary condition for the realization of the pump–dump process is, that at least some minor parts of the wavepacket reach the transition moment region in the excited state which leads to the target isomer in the ground state.

To facilitate a pump–dump mechanism, a long-range downchirp is used as the initial guess, such that a small fraction of the wavepacket is dumped in the Franck–Condon region of isomer C. The optimization leads to a laser pulse with the following features (see Fig. 4): a short pump pulse with an up-chirped frequency progression is followed by an intense dump pulse which consists of two main frequencies. This laser pulse causes the following dynamics of the wavefunction (see Fig. 5a)): during the excitation process, 81% of the population are transferred to the excited state where the wavefunction evolves in a very closed

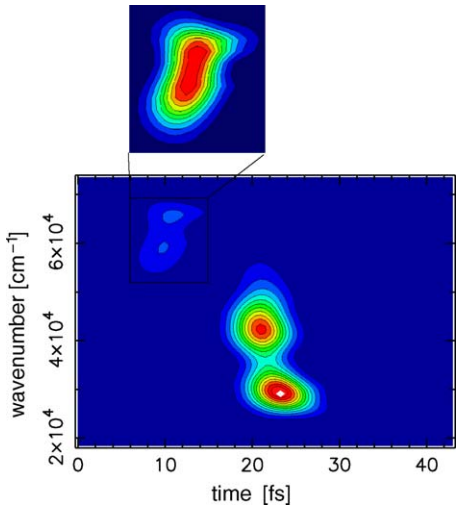

Fig. 4. XFROG representation of the optimized laser pulse including a zoom of the pump pulse.

form towards the Franck–Condon region of isomer C within few femtoseconds. There it localizes and 84% of the population in the excited state are dumped to the ground state of isomer C, leading to an absolute yield of 0.66. In our former control approach using an intermediate target, the absolute yield is just 0.27, although the relative yield of isomer C is 91% [25]. The small absolute value is mainly due to the parts of the wavepacket which remain in the excited state because this approach relies on the transfer through the conical intersections resulting in a stepwise relaxation mechanism. Only the first steps can be controlled, afterwards the control of the wavepacket is lost and the natural branching ratio reappears.

In the pump–dump mechanism, the wavepacket is guided through the dark region directly to the other transition moment region without crossing the conical intersections. To reach the transition region, the wavepacket needs an enhanced momentum

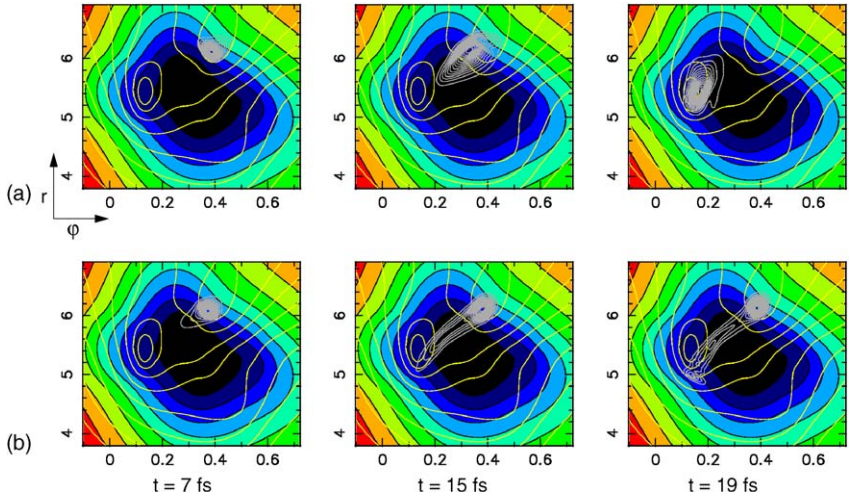

Fig. 5. Snapshots of the wavepacket in the excited state. The axes are given in Bohr. The white lines indicate the electronic ground state. (a) After excitation with the optimized laser pulse. (b) After excitation with a simple downchirp. Here the region of the transition dipole moment of isomer C is missed.

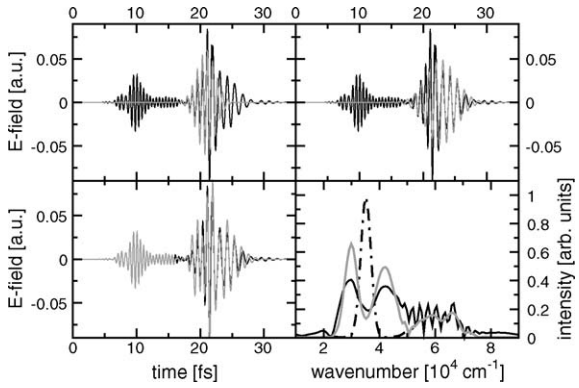

Fig. 6. The first three panels display the electric fields of the optimized pulse (black) and the reconstructed dump pulse consisting of two sub pulses with different frequencies (grey). The upper left panel shows the sub pulse of higher frequency, the upper right panel the sub pulse of lower frequency. The lower left panel shows the complete reconstructed pulse and the optimal field. The pump pulse cannot be reconstructed in a simple way and is therefore left unchanged. The corresponding DFT spectra are given in the lower right panel. The dumping can also be performed by a single Gaussian laser pulse (dotted line in the spectrum).

in φ, which is provided by the optimal shaped pump pulse. For comparison, the lower panels of Fig. 5 show the dynamics resulting after an excitation of the wavepacket by a simple downchirp laser pulse. Here the wavepacket misses the Franck–Condon region and therefore almost no dumping to the target region is possible, but the wavepacket stays in the excited state much longer and returns to the ground state via the conical intersections. Furthermore, the wavepacket is less localized, prohibiting an instantaneous dumping.

5. Analysis of the optimized pulse and reconstruction

The resulting optimized field has a rather complex form, but we will show that it is possible to simplify its structure. The XFROG representation (Fig. 4) reveals that the dump pulse exhibits two main frequencies. In addition, the DFT spectrum (Fig. 6, bottom right) reveals at higher frequencies (above 50,000 cm^{-1}) a complex structure for the pump pulse. Therefore we try a reconstruction of the dumping part of the pulse by two separate Gaussian laser pulses with the corresponding frequencies at the proper points in time. As they overlap in the time domain, the splitting of the dump pulse into two parts is done in the frequency domain. Back transformation into the time domain reveals the exact time occurrence of these frequency components. Both analyzed frequencies appear in the dump pulse and with less intensity in the pump pulse, too. Similarly, the frequencies of the pump pulse are present to some extent in the dump pulse. In the reconstruction of the optimized pulse sequence the pump pulse is left unchanged while the dump pulse is built up from the two leading frequencies only, neglecting the higher frequency components. The resulting dump pulse consists of two simple Fourier limited laser pulses with the correct relative phase with respect to each other and to the pump pulse. The upper graphs in Fig. 6 show these reconstructed pulses (grey lines) together with the optimized pulse (black curve). The third graph shows the laser field obtained by the addition of these Gaussian pulses and the unchanged optimal pump pulse. With this reconstructed laser pulse a quantum dynamical calculation is performed. Of course, the pumping process and the evolution of the excited state wavepacket are the same as in the optimized case. The reconstructed pulse dumps 82% of the excited wavepacket to the target region, which leads to an absolute population in the regime of isomer C of 0.62. Considering the simplicity of the reconstruction process, the target is reached very well. Fig. 7 shows the wavepackets in the ground state during the dump process. The smaller wavepacket in each picture represents the part of the initial wavefunction that was not excited by the pump pulse but remains in the minimum of isomer E (13%).

In previous investigations regarding molecular quantum gates a distinct sensitivity of the fidelity on the carrier-envelope phase (CEP) of the sub pulses was reported [33,34]. To examine the influence of the CEP in the present case we constructed dump pulses with different CEPs: first, the CEPs of both sub pulses were changed to the same amount, then the CEP of only one sub pulse was changed, leading to a different relative phase of the two sub pulses. The subsequent quantum dynamical calculations with these pulses revealed that the CEP has almost no influence on the dumping process. This means that pump and dump pulse could be generated by different laser sources, only the time delay has to be correct. Even a simple Gaussian dump pulse with a single main frequency and a FWHM of 7 fs (Fig. 6, right bottom panel, dotted line) leads to very good results: 77% of the excited state wavepacket are dumped, leading to an absolute population of isomer C of 0.60. We think that the pulse duration of the single dump pulse can be chosen longer, as long as the time delay to the pump pulse is correct and the intensity is not high enough to create Rabi oscillations.

In contrast, it was not possible to reconstruct the pump pulse with simple laser pulses. It has to act on the wavepacket in a very special way and to control the direction of the wavepacket's

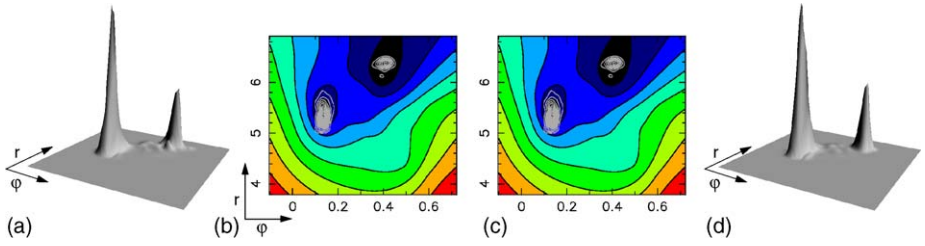

Fig. 7. Snapshots of the wavepackets in the ground state during the dump process. (a and b) The wavefunction dumped with the optimized pulse; (c and d) the wavefunction after dumping with the reconstructed pulse. All pictures are taken at $T = 22$ fs, i.e. after the maximum of the dump pulse.

motion. Therefore we used the phase-sensitive variant of the OCT algorithm to achieve full control over the wavepacket's movement [8]. Anyway, the spectrum of the reconstructed pulses is simpler also in the higher frequency regime (cf. Fig. 6, right bottom panel, grey curve), because the optimized dump pulse included frequencies in this regime which are not necessary and are therefore neglected in the reconstructed pulses. Nevertheless, a realization of the pump pulse seems possible as its mask function consists of 46 pixels and exhibits two main frequencies.

6. Conclusion and outlook

In this work, we presented an optimization scheme which can handle target definitions inside and/or outside a damping function. The target is also flexible with respect to time as the yield includes the sum over all parts of the wavefunction that have hit the target region during the propagation. With this scheme, a ground state target can be defined for photochemical reactions where vibrationally hot product states are formed intermediately, without the necessity to include relaxation into other modes in the system Hamiltonian. Thus, we can control the photochemical ring closure reaction from the ground state of isomer E via an excited electronic state exhibiting dark regions to the ground state of the product isomer C. When OCT is applied, the resulting optimized pulse follows a pump–dump sequence where the conical intersections are not involved. Our pulse analysis showed that it is possible to simplify the dumping part of the pulse significantly as its phase is not important, but mainly its frequency, intensity and time delay matter. This means that in principle different laser sources can be used to generate the pump–dump sequence. We think that a considerable simplification of the pump sequence is only possible when the wavepacket stays longer in the optically accessible region as it would be the case in a system with smoother electronic surfaces, i.e. with a smaller gradient. At least some of the various fulgide systems with enhanced masses and a stiffer framework should offer these conditions.

Another challenge is the optimization of the ring opening reaction from isomer C to isomer E. When using a ground state target the OCT algorithm always searches for an all optical pathway because this process is faster and easier to control than the relaxation through conical intersections. For the transfer from C to E, the transition region to the target cannot be reached, because the value of r in the ground state minimum and along the minimum energy path in the optically accessible region of the excited state hardly changes. Accordingly, the wavepacket gains no momentum in this direction and consequently a control of the motion along r, necessary to reach the Franck–Condon region of isomer E in the excited state, is not possible. Instead, the optimal pulse induces a pump–dump scheme in the Franck–Condon region of the educt followed by a ground state reaction pathway. In the case of the ring opening of cyclohexadiene this pathway has no equivalent in the experiment and violates the Woodward–Hofmann rules for the thermic ground state reaction. Therefore relaxation through the conical intersections is the only possible realistic pathway which means that an intermediate target has to be used in the theoretical approach.

The presented optimization scheme can also be used to define the flux of the nuclear wavefunction through a part of an electronic surface as target. In that case, parts of the wavefunction crossing the area of interest would have to be damped away and saved for the backward propagation. With our algorithm, the propagation time T can be chosen as long as computation time allows. Thus the control of a stepwise mechanism is possible as long as the wavefunction is accessible by laser light.

Acknowledgments

The authors would like to thank K.L. Kompa for continuous interest and support. The financial support of the DFG and the VCI is gratefully acknowledged. D.G. thanks the University of Munich, LMU, for a Ph.D. scholarship.

References

[1] B.L. Feringa (Ed.), Molecular Switches, Wiley, VCH, 2001.
[2] I.B. Ramsteiner, A. Hartschuh, H. Port, Relaxation pathways and fs dynamics in a photoswitchable intramolecular D → A energy transfer system, Chem. Phys. Lett. 343 (2001) 83–90.
[3] J.M. Endtner, F. Effenberger, A. Hartschuh, H. Port, Optical on/off switching of intramolecular photoinduced charge separation in a donor-bridge-acceptor system containing dithienylethene, J. Am. Chem. Soc. 122 (2000) 3037–3046.
[4] W. Zhu, J. Botina, H. Rabitz, Rapidly convergent iteration methods for quantum optimal control of population, J. Chem. Phys. 108 (5) (1998) 1953–1963.
[5] D. Tannor, S.A. Rice, Control of selectivity of chemical reaction via control of wave packet evolution, J. Chem. Phys. 83 (1985) 5013–5018.
[6] J. Manz, K. Sundermann, R. de Vivie-Riedle, Quantum optimal control strategies for photoisomerization via electronically excited states, Chem. Phys. Lett. 290 (1998) 415–422.
[7] K. Sundermann, R. de Vivie-Riedle, Extensions to quantum control algorithms and applications to special problems in state selective molecular dynamics, J. Chem. Phys. 110 (4) (1999) 1896–1904.
[8] D. Geppert, R. de Vivie-Riedle, Velocity control of ultrafast reactions: manipulation of the nuclear wave packets momentum with phase-sensitive Optimal Control Theory, Chem. Phys. Lett. 404 (2005) 289–295.
[9] T. Brixner, G. Gerber, Quantum control of gas-phase and liquid-phase femtochemistry, Chem. Phys. Chem. 4 (2003) 418–438.
[10] A. Assion, T. Baumert, M. Bergt, T. Brixner, B. Kiefer, V. Seyfried, M. Strehle, G. Gerber, Control of chemical reactions by feedback-optimized phase-shaped femtosecond laser pulses, Science 282 (1998) 919–922.
[11] J.L. Herek, W. Wohlleben, R.J. Cogdell, D. Zeidler, M. Motzkus, Quantum control of energy flow in light harvesting, Nature 417 (2002) 533.
[12] T.C. Weinacht, J.L. White, P.H. Bucksbaum, Toward strong field mode-selective chemistry, J. Phys. Chem. A 103 (1999) 10166–10168.
[13] R.J. Levis, G.M. Menkir, H. Rabitz, Selective bond dissociation and rearrangement with optimally tailored, strong-field laser pulses, Science 292 (2001) 709–713.
[14] M. Hacker, G. Stobrawa, R. Sauerbrey, T. Buckup, M. Motzkus, M. Wildenhain, A. Gehner, Micromirror slm for femtosecond pulse shaping in the ultraviolet, Appl. Phys. B 76 (2003) 711.
[15] C. Schriever, S. Lochbrunner, M. Opitz, E. Riedle, 19 femtosecond shaped ultraviolet pulses, Opt. Lett. 31 (4) (2006) 543–545.
[16] P.J. Reid, S.J. Doig, S.D. Wickham, R.A. Mathies, Photochemical ring-opening reactions are complete in picoseconds: a time-resolved UV resonance raman study of 1,3-cyclohexadiene, J. Am. Chem. Soc. 115 (11) (1993) 4754–4763.
[17] M.O. Trulson, G.D. Dollinger, R.A. Mathies, Excited state structure and femtosecond ring-opening dynamics of 1,3-cyclohexadiene from

absolute resonance raman intensities, J. Chem. Phys. 90 (8) (1989) 4274–4281.

[18] S. Lochbrunner, W. Fuß, W.E. Schmid, K.-L. Kompa, Electronic relaxation and ground-state dynamics of 1,3-cyclohexadiene and *cis*-hexatriene, J. Phys. Chem. A 102 (1998) 9334–9344.

[19] S.H. Pullen, N.A. Anderson, L.A. Walker II, R.J. Sension, The ultrafast photochemical ring-opening reaction of 1,3-cyclohexadiene in cyclohexane, J. Chem. Phys. 108 (2) (1998) 556–563.

[20] P. Celani, F. Bernardi, M.A. Robb, M. Olivucci, Do photochemical ring-openings occur on the spectroscopic state? $1B_2$ pathways for the cyclohexadiene/hexatriene photochemical interconversion, J. Phys. Chem. 100 (50) (1996) 19364–19366.

[21] P. Celani, S. Ottani, M. Olivucci, F. Bernardi, M.A. Robb, What happens during the picosecond lifetime of $2A_1$ cyclohexa-1,3-diene? A CAS-SCF study of the cyclohexadiene/hexatriene photochemical interconversion, J. Am. Chem. Soc. 116 (22) (1994) 10141–10151.

[22] M. Garavelli, P. Celani, M. Fato, M.J. Bearpark, B.R. Smith, M. Olivucci, M.A. Robb, Relaxation paths from a conical intersection: the mechanism of product formation in the cyclohexadiene/hexatriene photochemical interconversion, J. Phys. Chem. A 101 (11) (1997) 2023–2032.

[23] A. Hofmann, R. de Vivie-Riedle, Quantum dynamics of photoexcited cyclohexadiene introducing reactive coordinates, J. Chem. Phys. 112 (11) (2000) 5054–5059.

[24] A. Hofmann, R. de Vivie-Riedle, Adiabatic approach for ultrafast quantum dynamics mediated by simultaneously active conical intersections, Chem. Phys. Lett. 346 (2001) 299–304.

[25] D. Geppert, L. Seyfarth, R. de Vivie-Riedle, Laser control schemes for molecular switches, App. Phys. B 79 (2004) 987–992.

[26] C. Leforestier, R.H. Bisseling, C. Cerjan, M.D. Feit, R. Friesner, A. Guldberg, A. Hammerich, G. Jolicard, W. Karrlein, H.-D. Meyer, N. Lipkin, O. Roncero, R. Kosloff, A comparison of different propagation schemes for the time dependent schrodinger equation, J. Comp. Phys. 94 (1991) 59–80.

[27] G. Katz, R. Baer, R. Kosloff, A new method for numerical flux calculations in quantum molecular dynamics, Chem. Phys. Lett. 239 (1995) 230–236.

[28] R. Kosloff, D. Kosloff, Absorbing boundaries for wave propagation problems, J. Comp. Phys. 63 (1986) 363–376.

[29] A. Hofmann, L. Kurtz, R. de Vivie-Riedle, Interaction of electronic structure and nuclear dynamics on the s_1 reaction surface for the ring opening of cyclohexadiene, Appl. Phys. B 71 (2000) 391–396.

[30] K. Nakagami, Y. Ohtsuki, Y. Fujimura, Quantum optimal control of unbounded molecular dynamics: application to NaI predissociation, J. Chem. Phys. 117 (14) (2002) 6429–6438.

[31] D. Tannor, R. Kosloff, S.A. Rice, Coherent pulse sequence induced control of selectivity of reactions: exact quantum mechanical calculations, J. Chem. Phys. 85 (1986) 5805–5820.

[32] M. Abe, Y. Ohtsuki, Y. Fujimura, W. Domcke, Optimal control of ultrafast *cis–trans* photoisomerization of retinal in rhodopsin via a conical intersection, J. Phys. Chem. 123 (14) (2005) 144508.

[33] U. Troppmann, R. de Vivie-Riedle, Mechanisms of local and global molecular quantum gates and their implementation prospects, J. Chem. Phys. 122 (2005) 154105.

[34] B.M.R. Korff, U. Troppmann, R. de Vivie-Riedle, Manganese-pentacarbonyl-bromide as candidate for a molecular qubit system operated in the infrared regime, J. Chem. Phys. 123 (2005) 244509.